Scheduled state feedback control of a wind turbine

Engels, W. P.; Van Der Hoek, D.; Yu, W.; Reyes Baez, R.

DOI
10.1088/1742-6596/1618/2/022064

Publication date
2020

Document Version
Final published version

Published in
Journal of Physics: Conference Series

Scheduled state feedback control of a wind turbine

Scheduled state feedback control of a wind turbine

W. P. Engels[1], D. van der Hoek[2], W. Yu[1], R. Reyes Baez[1]

1 TNO, Westerduinweg 3, 1755 LE Petten, The Netherlands
2 TU-Delft, Mekelweg 5, 2628 CD Delft

wouter.engels@tno.nl

Abstract. Many wind turbines are still controlled using gain scheduled, PI(D) controllers. Another option is to use a state feedback controller, such as LQG control. However, for wind turbines that is not straight forward solution, because the system is non-linear and the impact of pitching on the states varies in time. This paper presents a variation on state feedback control. An Extended Kalman Filter is combined with gain scheduling of the state feedback gains depending on aero-dynamic sensitivities, which enables an approximation of non-linear control. This controller structure is intended to be used in more comprehensive controller optimisation studies. The scheduled state feedback controller shows good behaviour and can outperform the original PID controller.

1. Introduction

A wind turbine controller decides the balance between yield on the one hand and wind turbine loading, actuator effort and power quality on the other hand. Most modern wind turbine controllers behave dependent on the mean wind speed: in conditions below rated wind speed, wind turbines generally follow a basic control law, where the torque is set directly based on the rotor speed. If the wind speed is sufficiently high, the controller maintains the rotor speed at the rated-rotor speed by varying the pitch angle of the blades. This is commonly achieved by using a proportional–integral (PI) controller on the pitch angle [1], possibly also containing a derivative term (D). Because the effect of a change in pitch angle on the rotor speed is dependent on the pitch angle, the controller gain is scaled depending on the pitch angle. Also, the additional effects of dynamic inflow with respect to changes in pitch angle can be taken into account by filtering the desired pitch angle (or rate) with a pitch angle dependent filter [2]. In terms of control, the PI(D) controller is used to control a non-linear system, where the non-linearity of the control input on the system is considered and other non-linearities are ignored. This type of controller can perform well, especially if it is extended with further situation specific adaptions [3].

Other control algorithms take advantage of the known response of the wind turbine. These control algorithms are generally based on an estimate of this response. And, although the structural response is approximately linear, the aerodynamic interaction is not. Despite this non-linearity, state space control based on linearised estimation and control is possible, as was shown [4, 5]. Because the system is non-linear, a non-linear estimator, e.g. an extended Kalman filter or unscented Kalman filter [6], should give better estimates of the states than a linear filter.

These improved estimates can be used, simply as inputs to PI controllers or for state-based feedback control [7]. An example of state feedback control is Linear Quadratic Gaussian (LQG) (see e.g. [8]) control where Kalman state estimator is used, combined with a Linear Quadratic Regulator (LQR) control. If a system is known, observable, linear, time-invariant, and subject to white noise

disturbances and noise sources, the Kalman filter gives an optimal estimate of all the states [9]. Whereas the time-invariant feedback matrix calculated with LQR will optimally control the system to minimize a given quadratic cost function if the states of the system are exactly known and the system is controllable. For the wind turbine, the system is parameter varying and changing continuously. Logically, the associated state feedback matrix ought to change continuously as well. For any operating point, the model can be linearized and an LQR controller could be calculated and used, but doing so online would be challenging, both computationally and numerically. The scheduled controller approach is used to circumvent this issue.

(Non-linear) Model predictive control on the other hand takes the estimation one step further and tries to predict the optimal control action based on the evaluation of the cost function over a finite time horizon. Although model predictive control has shown promising results for wind turbines, especially when dealing with constraints, extreme loads and LIDAR based feedforward control (e.g. [10]) the advantages in normal, turbulent load cases are not clear.

In this paper, we explore the combination of an extended Kalman filter with a scheduled state-feedback controller design. Rather than calculating state feedback matrices at runtime, the matrices are calculated beforehand and then scheduled based a linear regression, this reduces the computational effort to a simple matrix multiplication. Although stability is not rigorously proven, simulations consistently show good behaviour in a fully non-linear aeroelastic simulation of normal turbulent wind and improved performance compared to the baseline controller.

2. Methodology

The following methodology is used to design the controller:

1) An Extended Kalman Filter is designed
2) The states of this filter are augmented with the integral of the rotor speed setpoint error
3) Locally stabilising, LQR state-feedback controllers are designed for different realisations of the states of the system.
4) These gains are then approximated with a linear regression to a set of selected predictors.
5) The results of the linear regression are then used in the controller to schedule the gains.

This scheduled state feedback controller (SSFC) is then tested on a full aero-elastic simulation using Phatas [11]. This method is tested on the Avatar wind turbine model [12], a modification of the Innwind 10 MW model [13] and compared to our current baseline controller.

3. Extended Kalman filter

As explained, the first step is to create an extended Kalman Filter from a non-linear analytical model. The work by Knudsen and Bak [14] is used for the dynamic inflow, but the model is extended with tower and drive train dynamics. Figure 1 shows the estimation of the rotor effective wind speed in comparison with our current estimator and the simulation. The improvement in the estimation is marked for larger changes of the aerodynamic torque. However, literature concerning Extended Kalman Filters does note that the robustness of this filter may be an issue (e.g. [15]), because the algorithm may underestimate the .

3.1. Main structural dynamics

The Kalman filter should be used to estimate the main dynamics of the system. Normally these constitute the lowest-frequency dynamics. Here, the 1st drive train frequency and the 1st tower frequency are included. The method described here can be extended to include more degrees of freedom.

The drive-train model is 1st degree model, describing torsional deformation γ in the drive train itself. The rotor speed Ω_r is driven by an aerodynamic torque T_a, the rotor is connected to a flexible shaft modelled as a stiffness and damping. The shaft drives the generator speed Ω_g which is also subject to a counter torque T_{gen}. The dynamics of the drivetrain can be modelled using the equations of motion given below; for brevity drive train loss factors have been omitted from these equations.

$$\dot{\gamma} = \Omega_r - \Omega_g^{SSE} \quad (1)$$
$$J_r\dot{\Omega}_r = -\mu_d\dot{\gamma} - k_d\gamma + T_a \quad (2)$$
$$i^2 J_g\dot{\Omega}_g^{SSE} = \mu_d\dot{\gamma} + k_d\gamma - iT_{gen} \quad (3)$$

Here J is used to denote the moment of inertia of the rotor and generator respectively. The parameter μ_d indicates the damping and k_d the stiffness of the drivetrain and i the gearbox ratio. Notice as well that the generator speed is given as the slow shaft equivalent (SSE), i.e., it has approximately the same magnitude as the rotor speed.

Like the drive train dynamics, the tower top fore-aft dynamics are described with the following equation:

$$M_t\ddot{d}_t = -\mu_t\dot{d}_t - k_t d_t + F_a \quad (4)$$

Where d_t is the tower top downwind displacement, M_t is the tower top equivalent mass, μ_t and k_t, respectively the tower equivalent damping and stiffness and F_a the axial force.

Finally, a basic integrator model is added for the pitch system, such that the system can be controlled using a pitch rate signal. A pitch rate signal is used, because the pitch rate can be weighted as a controller effort cost in the calculation of the LQR optimal controller, weighting the pitch angle would not be useful.

$$\theta = \frac{1}{s}\dot{\theta} \quad (5)$$

3.2. Aerodynamic model

The structural model is linear and time-invariant. The non-linearity lies in the aerodynamic forces and the coupling between the structural motions and aerodynamic loading.

As mentioned, the aerodynamic model used here is based on the work by Knudsen and Bak [8], the model describes the torque as function of the windspeed, but with a term based on the dynamic inflow dynamics. Other dynamic inflow models are available in literature, e.g. [16]. The model of Knudsen and Bak was chosen here, because the parameters needed are based directly on the power and thrust coefficients C_p and C_t, and a steady state inflow which can then easily be derived.

Instead it is computed at each time step based on the effective wind speed, which is given by:

$$v_r = v_m + v_t - \dot{d}_t \quad (6)$$

Where v_r is the effective rotor speed, v_m the mean wind speed, v_t a turbulent wind speed component and $\dot{d}_t$ the downwind tower velocity.

In order to also include the effect of dynamic inflow on the effective wind speed as was seen in Figure 2.3, a fictive wind speed is used to compute the aerodynamic torque as well as the axial force. This fictive wind speed is given by the following equation:

$$v_f = \frac{1-a_f}{1-a_s}v_r \quad (7)$$

Subsequently, the aerodynamic torque and axial force can be computed using:

$$T_a = \frac{1}{2}\rho\pi R^3 C_q(\lambda,\theta)v_f^2 \quad (8)$$
$$F_a = \frac{1}{2}\rho\pi R^3 C_t(\lambda,\theta)v_f^2 \quad (9)$$

For the controller design the model assumes the turbulent wind v_t is a random walk model driven by a random noise process.

3.3. Extended Kalman Filter

The Extended Kalman Filter (EKF) (see, e.g. [17]) requires several steps and assumes that we can write the dynamics of the system as:

$$x_k = f(x_{k-1}, u_{k-1}) + w_k \quad (10)$$
$$y_k = g(x_k) + v_k$$

Where f and g are non-linear functions and w and v describe stochastic disturbance and measurement noise terms respectively.

First, a-posteriori steps update the Kalman gain, and noise covariance on values from the previous timestep, the state estimates for the current time step k, based on current measurements, the estimates of the previous time step *k-1* and the calculated output for the previous time step. The second step estimates the states at the next time step, given the updated state estimates for the current time step. The steps are described using the following equations, where the vector $\hat{x}$ are the estimated states of the wind turbine, y the measured outputs of the system, and the matrix K gives the Kalman gain. Further, the function g is used to (non-linearly) calculate the estimated outputs. The matrix P is the covariance, C the jacobian of the output equation g and R represents the measurement noise covariance matrix. The subscript $k|k$ refers to the value at timestep k, as computed at timestep k.

Step 1: update of the Kalman gain:

$$K_k = P_{k|k-1}C_{k|k-1}^T(C_{k|k-1}P_{k|k-1}C_{k|k-1}^T + R)^{-1} \tag{11}$$

Step 2: update of the covariance matrix P

$$P_{k|k} = P_{k|k-1} - K_k C_{k|k-1}P_{k|k-1} \tag{12}$$

Step 3: update of state estimate based on the prediction at the previous time step and the current measurement:

$$\hat{x}_{k|k} = \hat{x}_{k|k-1} + K_k\left(y_k - g\left(\hat{x}_{k|k-1}\right)\right) \tag{13}$$

Step 4: a-priori estimate (or: prediction) of the state estimate at the next time step

$$\hat{x}_{k+1|k} = f\left(\hat{x}_{k|k}, u_k\right) \tag{14}$$

Step 5: a-priori estimate of the covariance matrix:

$$P_{k+1|k} = A_{k|k}P_{k|k}A_{k|k}^T + Q \tag{15}$$

Where, the function f evaluates the states computed by the non-linear system equations based on the updated system states from step 1. In this case the matrix A is the Jacobian of the state progress equation system matrix and Q indicates the process noise covariance and also follows the work by Bak.

When implementing the Extended Kalman Filter, it is important to initialise the states and the covariance matrix P well. The initial covariance matrix was based on the final value after the estimation had indeed converged to the appropriate values. To prevent the mentioned instability of the algorithm due to underestimation of the noise term, a small minimum noise term was included in the implementation.

4. LQR design and regression-based scheduling

4.1. LQR design

If the system was a linear, time-invariant system excited by white noise and quadratic cost, an LQR controller would be optimal. For a non-linear system, excited by non-white noise and a strongly non-linear cost function (e.g. the design equivalent load) LQR controller cannot be expected to be optimal. However, it must at least be stable in a region close to the operating point and therefore LQR is used as a starting point for the scheduled state feedback controller. As mentioned, the goal is to create a set of LQR gains, which are then scheduled based on certain parameters.

For a particular operating point, the LQR gains K_{LQR} are used to calculate a control action (pitch rate) at time step *k* according to:

$$\dot{\theta}_k = K_{LQR}\hat{x}_k \tag{16}$$

Where $\hat{x}_k$ denotes a vector of the estimated states. The linear quadratic K_{LQR} minimizes a quadratic cost function *J*:

$$J = x^T Q x + u^T R u \tag{17}$$

Where the matrix Q is used to assign cost to various states and the matrix R is used to weight the control effort. For the linear system:

$$\begin{aligned} x_k &= Ax_{k-1} + Bu_k + w_k \\ y_k &= Cx_k + Du_k + v_k \end{aligned} \tag{18}$$

These linearised models are generated near selected operating points to calculate the gains.

In addition to the states associated with the structural and aerodynamic model, one additional is state is added, which is the integral of the rotor speed error. This ensures that the controller can accurately track the desired rotor speed. Finally, the Q matrix weights the rotor speed tracking error, the integral of the rotor speed tracking error and the tower displacement.

Because of the non-linearity of the system, the linearised models are different for different rotor speeds, wind speeds, etc. Therefore, to create a sensible input set for the regression, deviations from the operating states are assumed that are random, but of realistic magnitude. LQR gains are then calculated for the linearised models at these random realisations. The random variations were distributed flatly within selected boundaries. Figure 2 shows the LQR gains for two states for given mean wind speed (along the x-axis), with variations in the turbulent wind speed and induced velocity. It should be noted that due to different sensitivities of torque and axial force to pitch actions and variations of the wind, the ratio between pitch activity and loads also varies for different conditions. This means that given selected weights for the states and the control effort, the minimized costs associated with each state or the input effort also varies with wind speed.

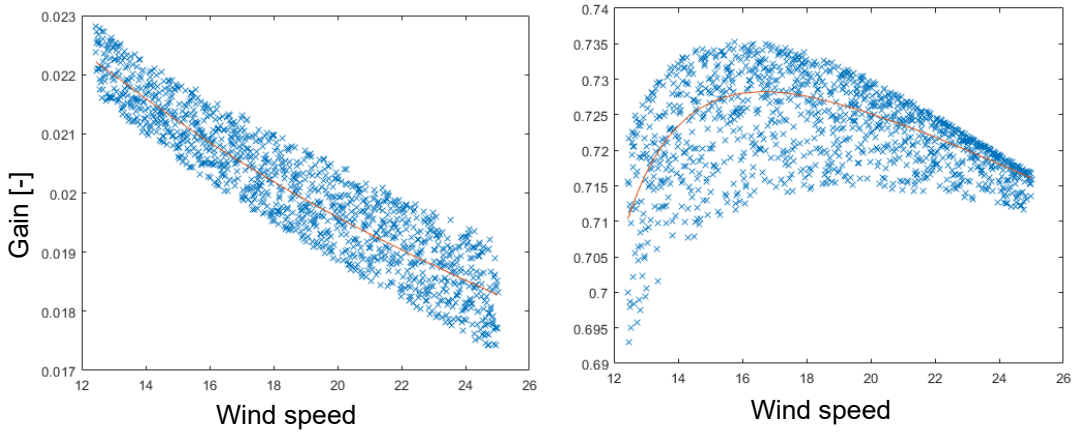

Figure 1: Calculated LQR gains (blue crosses) for different state realisations and the regression-based results (red line) for varying wind speeds (x-axis). The gains for two different states are shown.

4.2. Regression of LQR gains and scheduling

The set of gains calculated for variations in the model is used as input data for a linear regression with a selected set of predictors. The idea behind basing the gains on predictors is that the gains can also be calculated across a large operational range, to include, for instance, when the wind turbine is operating at reduced maximum power. A linear regression is used rather than a simple quadratic fit, because overfitting can be prevented more easily.

The predictors are selected from parameters that are already needed for the extended Kalman Filter or could easily be calculated from these parameters. The set is reduced to only include those parameters that are needed to obtain an accurate fit of the data. This parameter set consists of the wind speed V_w and a small number of aerodynamic sensitivities. In particular:

$V_w, \frac{\mathrm{d}C_q}{\mathrm{d}\theta}, \frac{\mathrm{d}C_t}{\mathrm{d}\theta}, \frac{\mathrm{d}a}{\mathrm{d}\theta}, V_w\frac{\mathrm{d}C_q}{\mathrm{d}\theta}, V_w\frac{\mathrm{d}C_t}{\mathrm{d}\theta}$ and $V_w\frac{\mathrm{d}a}{\mathrm{d}\theta}$.

where a is the static induction. The regression results in a matrix K_{reg} and a set of constant values, or offsets, $K_{offsets}$ for the various elements of the approximated $\widehat{K}_{LQR}$. This allows us to calculate the approximated $\widehat{K}_{LQR}$ as:

$$\widehat{K}_{LQR} = K_{reg} v_s + K_{offsets} \tag{19}$$

Where v_s is a vector of the parameters mentioned above. This means that by using the regression, gains were calculated by adding and multiplying 8 real values, with values that were already available, because they are required for the extended Kalman filter anyway. Computationally, this compares very

favourably to solving the discrete time algebraic Riccati equation for the linearised model at each time step.

The results of two such regressions are shown in figure 1. The red lines are the gains calculated at the operating point, without variations in the turbulent field and induction. It should be noted, that these gains vary differently with wind speed. Conventional gain scheduling of the pitch response of the controller output would not have been able to account for this and therefore not have been optimal for scheduling the LQR gains.

Given that this matrix is an approximation of the true LQR gains, this may introduce stability issues. Therefore stability of the scheduled gains was first verified using the linearised models, before simulating the controller with a fully-non-linear, aero-servo-elastic code Phatas [11] to show its effectiveness. Please note that this approach does not guarantee stability.

5. Simulation results

As mentioned in the introduction, a wind turbine controller must balance different objectives. Specifically, for this controller we analyse the following criteria:

1) The mean power production
2) The design equivalent load of the out-of-plane blade root bending moment
3) The design equivalent load of the tower fore-aft tower bottom bending moment
4) The pitch effort; the pitch duty cycle specifically

The design equivalent loads are calculated with appropriate material exponents for the tower, (steel, exponent 4) and the blade (glass-fibre reinforced epoxy, 10), while the pitch duty cycle is defined as the average absolute value of the instantaneous pitch rate multiplied with the instantaneous blade root bending moment. Because friction in bearings is commonly proportional to the out-of-plane loading (amongst other loads), the pitch duty cycle can be seen a measure of the power the pitch drives loose due to friction in the bearings.

The scheduled state feedback controller (SSFC) is compared to a baseline controller. The baseline controller is PD controller with pitch rate as output, which is similar to a PI controller on the blade angle. Gain scheduling is applied based on wind speed, rotor speed and pitch angle.

The controllers are simulated at three different wind speeds (17, 18 and 19 m/s), for two different seeds at each wind speed. These windspeeds were chosen to ensure that any differences between the controllers was not due to transitions from full-load to partial-load and vice-versa.

Finally, to create a fair performance comparison, the control effort must also be examined. This can be achieved by varying the control effort weighting in the calculation of the LQR matrices.

5.1. Filtering needed

Initial simulations showed that it is necessary to filter out excitations at frequencies 3, 6 and 9 multiples of the rotor speed. Otherwise the simulation results in significant additional pitch effort without any particular benefit to blade or tower loads. The filtering was applied between the EKF and the scheduled gains, and to all states equally. The same filters were applied in the baseline controller, to ensure a 'like with like' comparison as much as possible.

5.2. Results for the performance criteria

Figure 2 shows the performance criteria for the baseline controller (red star) and scheduled state feedback control based for varying input effort weightings. The power loss shown in figure 2 is the difference of the mean power during the simulations and rated power. Based on the values shown here, the state space controller marked in green is chosen as the best performing state-space controller.

In terms of energy, the chosen state feedback controller loses some energy compared to the baseline controller, the difference is about 21kW (approximately 0.2% of rated power). The difference is due a slightly lower mean rotor speed for the scheduled state feedback controller. It also should be noted that at lower pitch duty cycles (higher weighting of the pitch effort), the mean power loss of the

state-space controller is significantly higher and falls outside the chosen limits for the plot. The pitch duty cycle at this point is 26% lower than the baseline controller.

Both the design equivalent tower bottom bending moment and the blade root bending moment are reduced as well, by 2.7% and 4.2% respectively.

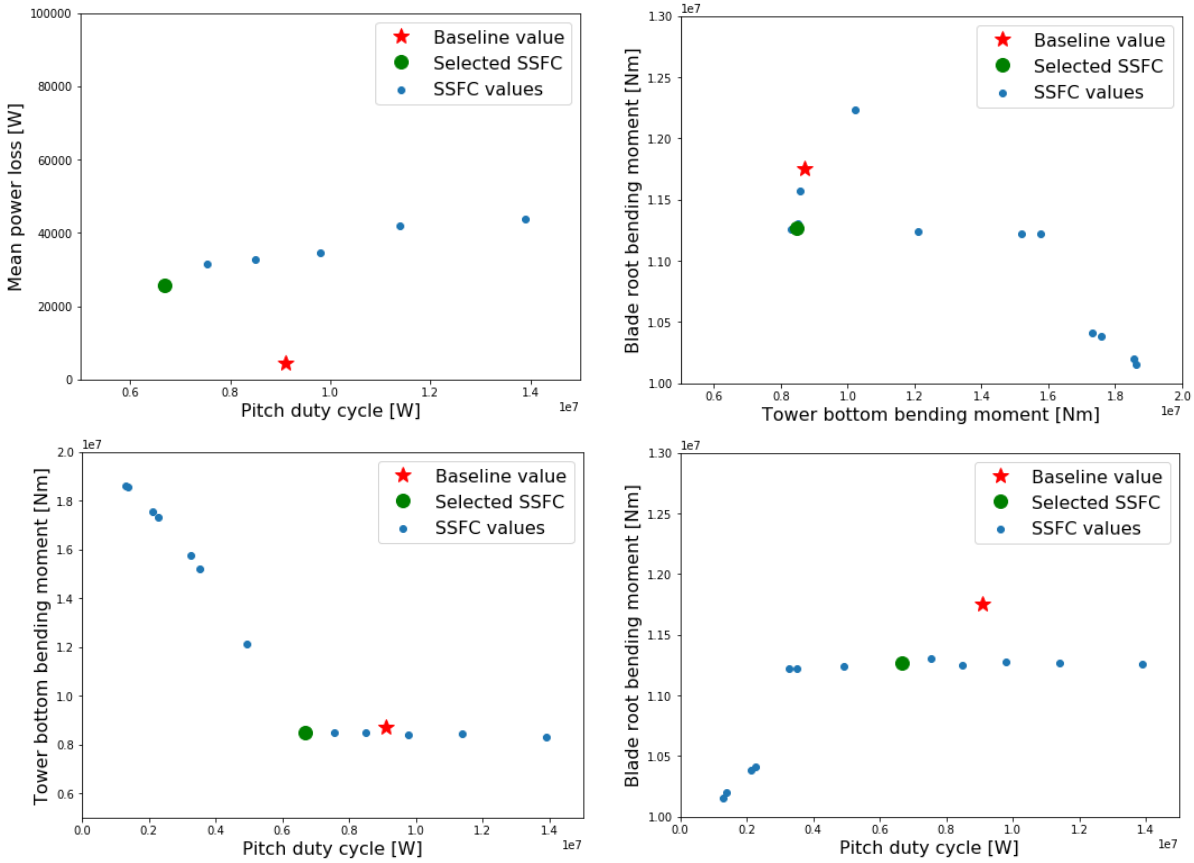

Figure 2: Performance criteria for baseline control and scheduled state feedback control (SSFC) for various weightings of the control effort

5.3. Time series comparison

For the comparison of the time-series, one of the time series at 18 m/s was selected. Figure 3 shows the time series of the baseline and the scheduled state feedback controller, for the rotor speed, the blade root bending moment, the pitch angle and the pitch rate.

The slightly higher mean rotor speed of the baseline controller is not immediately evident. For this time series, the mean rotor speed for the baseline controller was 9.59 rpm, the state-space controller achieved 9.57 rpm, whereas the rated rotor speed is 9.60 rpm. The figure also shows that the baseline controller has higher amplitude rotor speed excursions.

The lower pitch activity is clearly visible. The time series of the pitch angle also show smoother pitch activity, with lower overshoots in the pitch angle.

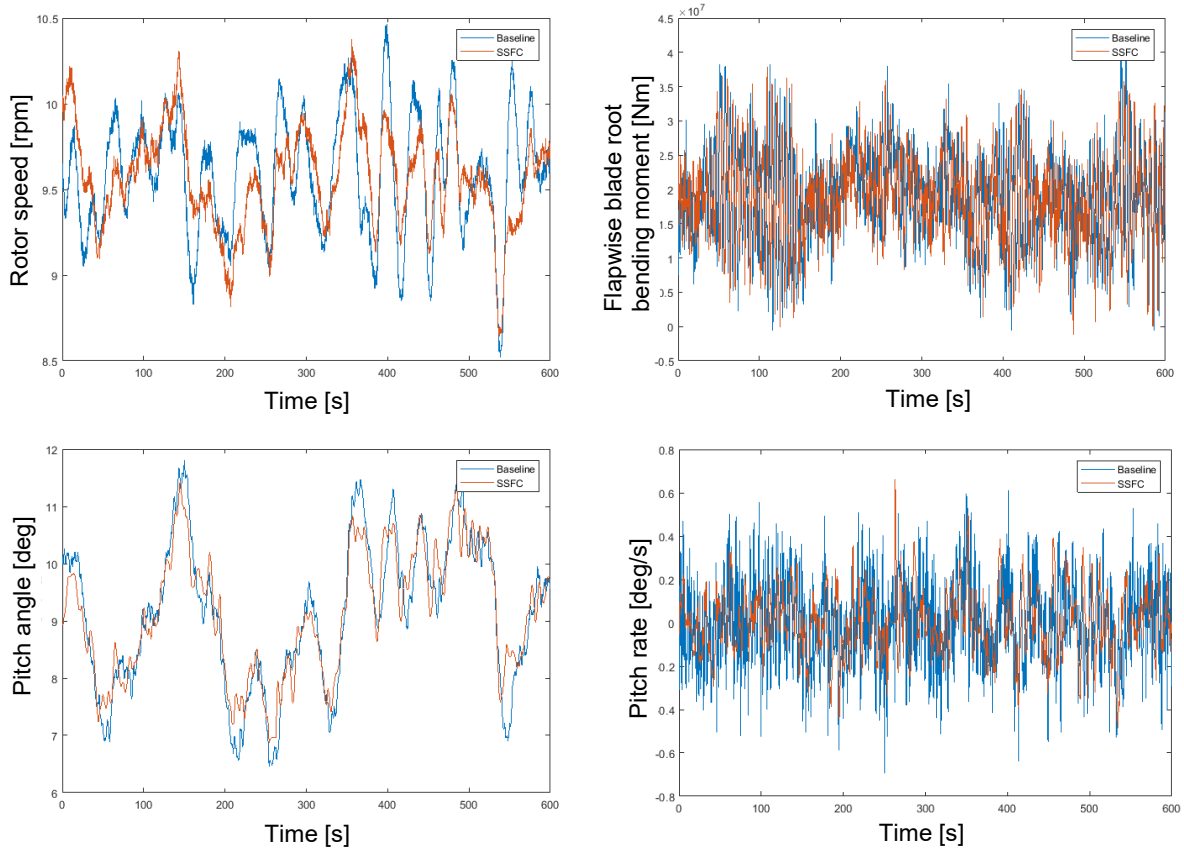

Figure 3: Time series comparison for baseline control and scheduled state feedback control.

6. Discussion, Conclusions and future work

6.1. Discussion

The variation in performance due to the weighting of the pitch effort is significant and must be done with care. And although the results show it is possible to design a scheduled state feedback controller that improves performance in most aspects with respect to the default PI(D) controller. However, the actual criteria for control are not quadratic and severely non-linear. This means that the gains calculated with LQR are unlikely to be truly optimal for these criteria and can probably be tuned to further improve performance.

6.2. Conclusions

A variation on the LQG controller structure was presented here that can handle non-linear changes in state feedback control gains effectively and computationally efficiently. Using the regression, gains were calculated by multiplying 8 real values, with values that were already available, because they were required for the extended Kalman filter anyway. The combination of extended Kalman filtering and the scheduled state-feedback controller resulted in a well performing controller, although strict stability remains to be proven. The results show improved performance relative to the default baseline controller, with a 4% reduction of the blade loads at a 26% lower duty cycle.

The scheduled state feedback controller is mainly intended as a structure for and a starting point from which the performance can be further optimised using other approaches; in particular by using Multi-Objective Bayesian Optimisation, such as described in [18].

6.3. Future work

Future work can focus on a number of aspects:

- extended proof of stability
- the further tuning of scheduled state feedback controllers
- the performance over a wider range of load cases
- robustness of the scheduled state feedback control to allow industrial application
- a more extensive structural model
- comparing performance based on unscented Kalman filters and the current extended one

Acknowledgement

The authors gratefully acknowledge the funding provided by the Dutch Government in the research project 'WT Brain'.

References

[1] E. Bossanyi, "The design of closed loop controllers for wind turbines," *Wind Energy,* vol. 3, pp. 149-163, 2000.

[2] T. van Engelen and E. van der Hooft, "Dynamic inflow compensation for pitch controlled wind turbines," in *Proceedings of EWEC*, 2004.

[3] W. Engels, S. Kanev, F. Savenije and D. Wouters, "ACT: Advanced Control Tool," in *European Wind Energy Association* , Vienna, 2013.

[4] K. Stol and J. Fingersh, "Wind Turbine Field Testing of State-Space Control Designs," NREL, Golden, Colorado, 2003.

[5] P. Fleming, A. Wright and J. van Wingerden, "Comparing State-Space Multivariable Controls to Multi-SISO Controls for Load Reduction of Drivetrain-Coupled Modes on Wind Turbines through Field-Testing Preprint," in *the 50th AIAA Aerospace Science Meeting*, Nashville, Tennessee, 2012.

[6] S. J. Julier, J. K. Uhlmann and H. F. Durrant-Whyte, "A New Approach for Filtering Nonlinear Systems," in *Proceeding of the American Control Conference*, Seattle, 1996.

[7] K. T. Magar, M. Balas, S. Frost and N. Li, "Adaptive State Feedback - Theory and Application for Wind Turbine Control," *Energies,* vol. 10, no. 12, 2017.

[8] S. Skogestad and I. Postlethwaite, Multivariable feedback control, John Wiley and Sons Ltd., 2005.

[9] R. Kalman, "A New Approach to Linear Filtering and Prediction Problem," *Journal of Basic Engineering,* vol. 82, pp. 35-45, 1960.

[10] S. Gros and A. Schild, "Real-time Economic Nonlinear Model Predictive Control for Wind Turbine Control," *International Journal of Control,* vol. 90, no. 12, pp. 2799-2812, 2017.

[11] C. Lindenburg, "Phatas User's Manual," WMC, Wieringerwerf, the Netherlands, 2018.

[12] A. G. Salcedo, R. Martín-San-Román, N. Lampropoulos, A. Barlas, G. Seros, J. Prospathopoulos, D. Manolas, L. Sartori, E. Jost, T. Maeder and F. Savenije, "AVATAR Deliverable 1.7:Evaluation of the new design: Advanced Reference Wind Turbine," 2017.

[13] C. Back, F. Zahle, R. Bitsche, T. Kim, A. Yde, L. C. Henriksen, A. Natarajan and M. Hansen, "Description of the DTU 10 MW Reference Wind," DTU Wind Energy, 2013.

[14] T. Knudsen and T. Bak, "Simple Model for Describing and Estimating Wind Turbine Dynamic Inflow.," in *American Control Conference*, Washington, USA, 2013.

[15] R. J. Fitzgerald, "Divergence of the Kalman Filter," *IEEE Transaction on Automatic control,* vol. AC 16, no. 6, pp. 736-747, 1971.

[16] H. Snel and J. Schepers, "Joint investigation of dynamic inflow effects and implementation of an engineering method," ECN, 1995.

[17] B. D. Anderson and J. B. Moore, Optimal Filtering, Englewood Cliffs: Prentice-Hall, 1979.

[18] W. Yu, W. Engels and C. Stock-William, "A Comparison of Multi-Objective Optimisation of Two Wind Turbine Control Desigs," in *Torque 2020 (submitted)*, Delft, 2020.